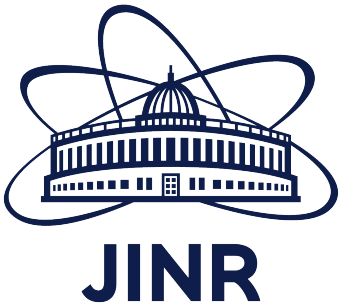

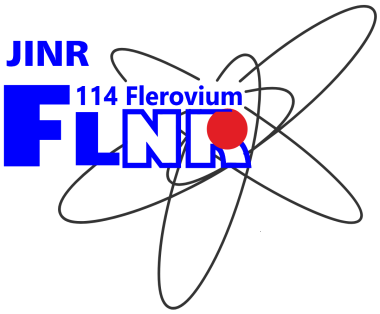

The Joint Institute for Nuclear Research
Flerov Laboratory of Nuclear Reactions
Chemistry of Transactinides

FINAL REPORT ON THE START PROGRAMME

Photodisintegration of the Isotope ^{106}Cd

Supervisor:
Dr. Rasulova Fazilat

Student:
Ikrom Ergashov, Uzbekistan
New Uzbekistan University

Participation period:
July 06 - August 16,
Summer Session 2025

Dubna, 2025

Contents

Abstract

In order to provide experimental constraints for p-process nucleosynthesis, this work examines the photodisintegration of the isotope ^{106}Cd, with particular attention to the (γ, n) and (γ, p) reactions. This study was conducted at the MT-25 microtron, where natural cadmium targets were exposed to bremsstrahlung radiation with electron energies ranging from 10 to 23 MeV. A high-purity germanium detector was used to measure the gamma-ray spectra, and the yields were normalised to the incident electrons. Characteristic γ-rays were used to determine the activity of ^{105}Cd ($T_{1/2}$ = 55.5 min) and ^{105}Ag ($T_{1/2}$ = 41.29 d), which showed notable discrepancies between experimental yields and theoretical predictions from TALYS-2.0 codes. Potentially as a result of nuclear structure effects close to the Z = 50 shell closure, the (γ, p) channel showed yields that were up to an order of magnitude higher than theoretical estimates. These results highlight the need for more experimental data and improved nuclear models to enhance p-process nucleosynthesis calculations.

Introduction

One of the most unresolved issues in nuclear astrophysics is the nucleosynthesis of proton-rich p-nuclides. Both the slow (s) and rapid (r) neutron capture processes avoid the mass region occupied by these 35 neutron-deficient stable isotopes, which range from ^{74}Se to ^{106}Hg [1]. According to current astrophysical models, p-nuclides are primarily created by a series of photodisintegration reactions, which include (γ, n), (γ, p), and (γ, α). These reactions are thought to occur at temperatures of ~2–3 GK during supernova explosions or pre-supernova stages [2]. Calculated and observed p-nuclide abundances continue to differ by up to two orders of magnitude despite major theoretical advancements, especially for isotopes such as ^{92,94}Mo [3]. The two main causes of these discrepancies are (1) uncertainties in the initial nuclear composition at the beginning of the p-process and (2) imprecise photonuclear reaction cross-sections used in nucleosynthesis calculations [4]. The latter restriction is particularly significant for reactions involving proton emission channels, for which there is currently a dearth of experimental data.

The cadmium isotopes ^{106}Cd and ^{108}Cd are two of the more intriguing examples of p-nuclides. Prior measurements with natural cadmium targets [5] only yielded combined cross-sections $((\gamma, n)+(\gamma, np)$ and $(\gamma, 2n)$ without isotopic resolution. With an integrated cross-section of 226 mb and a giant dipole resonance centred at 15.8 MeV with a width of 6.3 MeV, these data were added to the RIPL database [6] and are used as input for statistical model computations. This was enhanced by subsequent gamma-activation investigations [7, 8], which measured relative yields for individual reactions; however, absolute cross-sections for particular channels were not ascertained.

Photoproton reaction yields for ^{106}Cd are an order of magnitude higher than predicted by statistical models, according to experimental results [9]. This disparity highlights how important it is to measure every photodisintegration channel precisely, with a focus on proton-emitting reactions that might be more important in p-process nucleosynthesis than is currently taken into account in astrophysical models. The current study fills this gap by providing new experimental constraints for p-process nucleosynthesis calculations through comprehensive gamma-activation measurements of photonuclear reactions on cadmium isotopes.

Materials and Methods

2.1 Experimental setup and procedures

This investigation was conducted using the electron beam output from the MT-25 microtron [10], a high-precision accelerator capable of delivering stable electron beams. The electron energies were varied between 10 and 23 MeV in precise 1 MeV increments to systematically explore the energy dependence of the photonuclear reactions under study. To generate γ-radiation via bremsstrahlung, a 3 mm thick tungsten target was employed as the radiator. Tungsten was selected due to its high atomic number and density, which maximize photon production in the energy range of the giant dipole resonance (GDR), a dominant feature in photonuclear yieldss from the nucleon separation threshold (8 MeV) to approximately 20–30 MeV. To ensure a clean bremsstrahlung beam, a 30 mm thick aluminum absorber was positioned immediately behind the tungsten converter to remove residual electrons, thereby preventing contamination of the γ-ray spectrum. The irradiation targets, composed of natural cadmium, were tailored to the energy range: 10×10×0.5 mm for electron energies of 10–19 MeV and 5×5×0.5 mm for 20–23 MeV, optimizing the interaction volume for higher-energy photons. These targets were placed 1 cm from the tungsten converter to maximize exposure to the bremsstrahlung flux while maintaining spatial precision in the experimental geometry.

Beam current variations were meticulously monitored using a combination of a Faraday cup and a calibrated ionization chamber positioned within the beamline. The Faraday cup provided real-time measurements of the electron current during irradiation, while the ionization chamber offered complementary data on beam stability. The collected electrical charge on the target was digitized using a high-resolution analog-to-digital converter card, and the resulting data were logged into a web-accessible database via LabView software [11], ensuring robust data management and accessibility for subsequent analysis.

To further calibrate the accelerator current, the yield of the well-characterized ^{65}Cu(γ,n)^{64}Cu reaction was measured experimentally. A 0.15 mm thick cop-

per monitor foil was placed behind the irradiated cadmium target, chosen for the reliable and precisely measured yields of the ^{65}Cu(γ,n)^{64}Cu reaction [12]. The bremsstrahlung spectrum was modeled using Geant4 simulations [13], which provided a detailed representation of the photon energy distribution and enabled accurate yield calculations. The primary experimental parameters, including beam energy, target dimensions, and monitor foil specifications, are summarized in Table1.

Table 1: The main parameters of the experiments

Energy of electron (MeV)	Mass of cadmium target (mg)	Integral charge (mC)	Integral number of electrons incident on the tungsten converter ($\times 10^{16}$ particle)	Irradiation time (min)	Total measuring time of spectra (h)
10	475.6	50 ± 5	31 ± 3	97	44
11	447.8	50 ± 5	31 ± 3	150	44
12	454.5	50 ± 5	31 ± 3	125	44
13	451.0	50 ± 5	31 ± 3	155	47
14	451.2	30 ± 3	19 ± 2	175	39
15	413.8	20 ± 2	13 ± 1	65	41
16	427.2	10 ± 1	6.2 ± 0.6	65	40
17	427.4	4.0 ± 0.4	2.5 ± 0.3	37	39
18	401.5	3.0 ± 0.3	1.9 ± 0.2	24	36
19	389.3	3.0 ± 0.3	1.9 ± 0.2	32	39
20	113.6	3.0 ± 0.3	1.9 ± 0.2	51	39
21	116.3	3.0 ± 0.3	1.9 ± 0.2	35	37
22	115.8	3.0 ± 0.3	1.9 ± 0.2	27	40
23	112.0	3.0 ± 0.3	1.9 ± 0.2	21	40

Following irradiation, the cadmium targets were carefully transported to a dedicated low-background measurement room once radiation levels in the experimental hall were confirmed safe, adhering to strict radiation safety protocols. The induced activity in the irradiated targets was measured using a high-purity germanium (HPGe) γ-detector, which offered a resolution of 16 keV at 1332 keV, ensuring high sensitivity to the γ-ray emissions from activated isotopes. The detector was coupled with a 16K ADC/MCA (Multiport II Multichannel Analyzer, CANBERRA) and standard nuclear measurement electronics to achieve precise spectral analysis. Calibration of the HPGe detector's energy and efficiency was performed using standard γ-ray sources, ensuring accurate identification and quantification of the induced activity.

This setup allowed for the reliable detection of γ-rays emitted from the acti-

vated cadmium isotopes, providing critical data on the photonuclear reaction yields. A detailed account of the γ-activation measurement methodology, including detector calibration and data analysis procedures, is provided in references [14, 15]. These references also elaborate on the techniques used to minimize background noise and optimize the signal-to-noise ratio, which were essential for the high-precision measurements conducted in this study.

2.2 Yields of the reaction

The experimental yields of photonuclear reactions, denoted as Y_{exp}, were normalized to one electron of the accelerated beam incident on the bremsstrahlung target. These yields were calculated using the following expression:

$$Y_{\text{exp}} = \frac{S_p C_{\text{abs}}}{\varepsilon I_\gamma} \cdot \frac{t_{\text{real}}}{t_{\text{live}}} \cdot \frac{1}{N} \cdot \frac{1}{N_e} \cdot \frac{e^{\lambda t_{\text{cool}}}}{1 - e^{-\lambda t_{\text{real}}}} \cdot \frac{\lambda t_{\text{irr}}}{1 - e^{-\lambda t_{\text{irr}}}}, \tag{1}$$

where S_p represents the area under the full-energy peak in the gamma-ray spectrum, ε is the detector efficiency for the full-energy peak, I_γ denotes the probability of gamma emission for the transition of interest, C_{abs} is the correction factor for self-absorption of gamma rays within the sample, t_{real} and t_{live} are the real and live times of the measurement, respectively, N is the number of atoms in the activation sample, N_e is the total number of incident electrons, λ is the decay constant of the radioactive isotope, t_{cool} is the cooling time between irradiation and measurement, and t_{irr} is the duration of irradiation.

The theoretical yields, Y_{theor}, were obtained by convolving the yields of photonuclear reactions $\sigma(E)$ with the energy distribution density of bremsstrahlung photons per incident electron, $W(E, E_{\text{ymax}})$. For a natural mixture of isotopes, the yield accounts for contributions from all possible reactions producing the studied isotope:

$$Y_{\text{theor}} = \sum_i \alpha_i \int_{E_{\text{th}}}^{E_{\text{ymax}}} Y_i(E) W(E, E_{\text{ymax}})\, dE, \tag{2}$$

where E_{ymax} is the maximum kinetic energy of electrons striking the tungsten radiator, E is the energy of bremsstrahlung photons generated at the radiator, E_{th} is the energy threshold of the photonuclear reaction under study, α_i is the fractional abundance of the i-th isotope in the natural cadmium mixture, and $Y_i(E)$ is the yields of the i-th reaction contributing to isotope production. In this study, each radioactive nucleus was primarily formed via a single photonuclear reaction. Contributions from multiparticle reactions, evaluated using the TALYS-2.0 code, were found to be less than 1, indicating their negligible impact on the total yield.

Results and Discussion

3.1 Relative yields of the reactions (γ, n) and (γ, n) on the ^{106}Cd

Fig. 1 shows an example of the spectrum that can be gotten by using this method. This spectrum shows the lines that show the decays of the products that come from reactions on the isotopes of cadmium. Most of the lines in the detected spectra, on the other hand, come from the decays of nuclei that were made when heavier cadmium isotopes reacted with other elements.

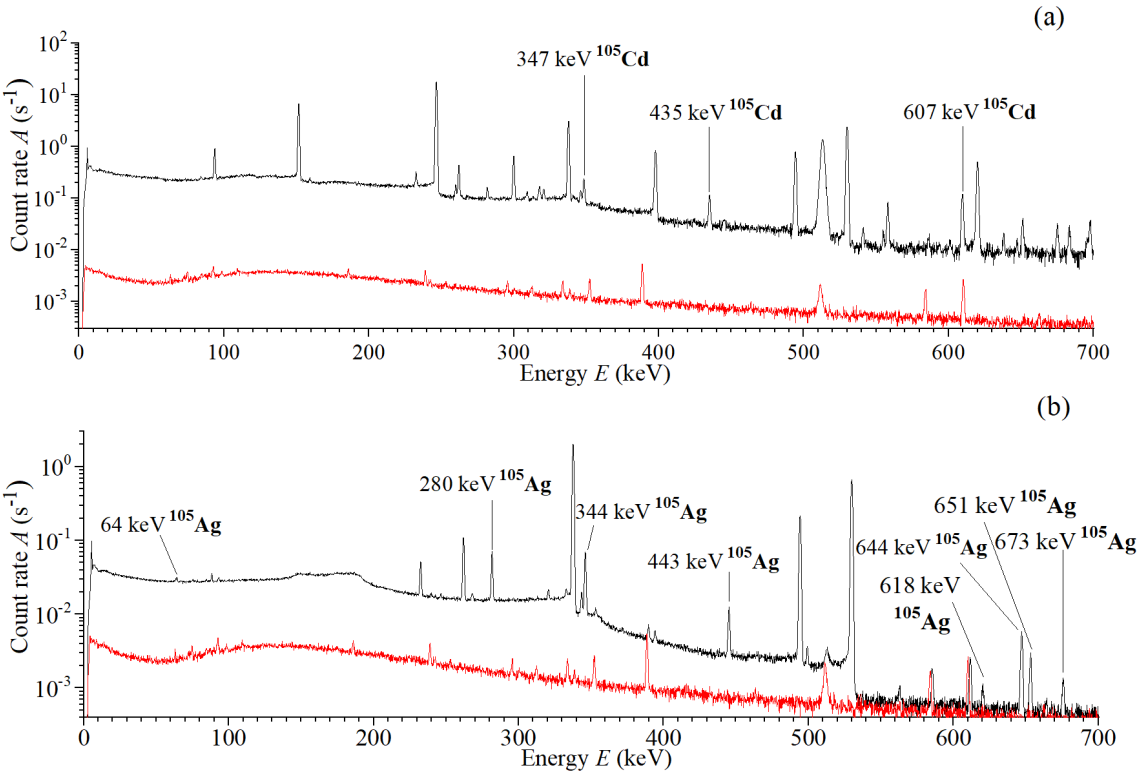

Figure 1: Induced-activity γ-rays spectrum of the cadmium target after the complation of irradiation

We aimed to measure four reaction channels for ^{106}Cd(γ, X): (γ, n), (γ, p), $(\gamma, 2n)$, and (γ, d). Table 2 lists their products and properties. Due to the high threshold energies of the $(\gamma, 2n)$ and (γ, d) reactions, only the (γ, n) and

(γ, p) channels were measured.

The nuclear decay schemes Fig. 2 of ^{105}Ag and ^{105}Cd were constructed using experimental data obtained from the **NuDat 3.0 database** (National Nuclear Data Center, NNDC). Energy levels, spin-parity assignments, lifetimes, transition multipolarities, and branching ratios were extracted from NuDat. Using these data, the decay scheme was manually drawn to clearly illustrate the level structure and transition patterns between the states of both nuclei.

Table 2: Reaction products and properties for ^{106}Cd(γ, X) reactions

Reaction product	Reaction	E_{th}, MeV	γ-ray energy, E_γ/keV (I/%)	Half-life
^{105}Cd	(γ, n)	10.87	346.87 (4.2), 961.84 (4.69) 1302.46 (3.98), 1388.48 (2.7)	55.4 m
^{105}Ag	(γ, p)	7.35	280.54 (31), 344.61 (42) 443.44 (10.9), 644.63 (10.2)	41.3 d
^{104}Cd	$(\gamma, 2n)$	19.3	83.5 (47), 709.3 (19.5)	57.7 m
^{104}Ag	(γ, d)	15.16	555.8 (92.6), 767.6 (65.7)	69.2 m

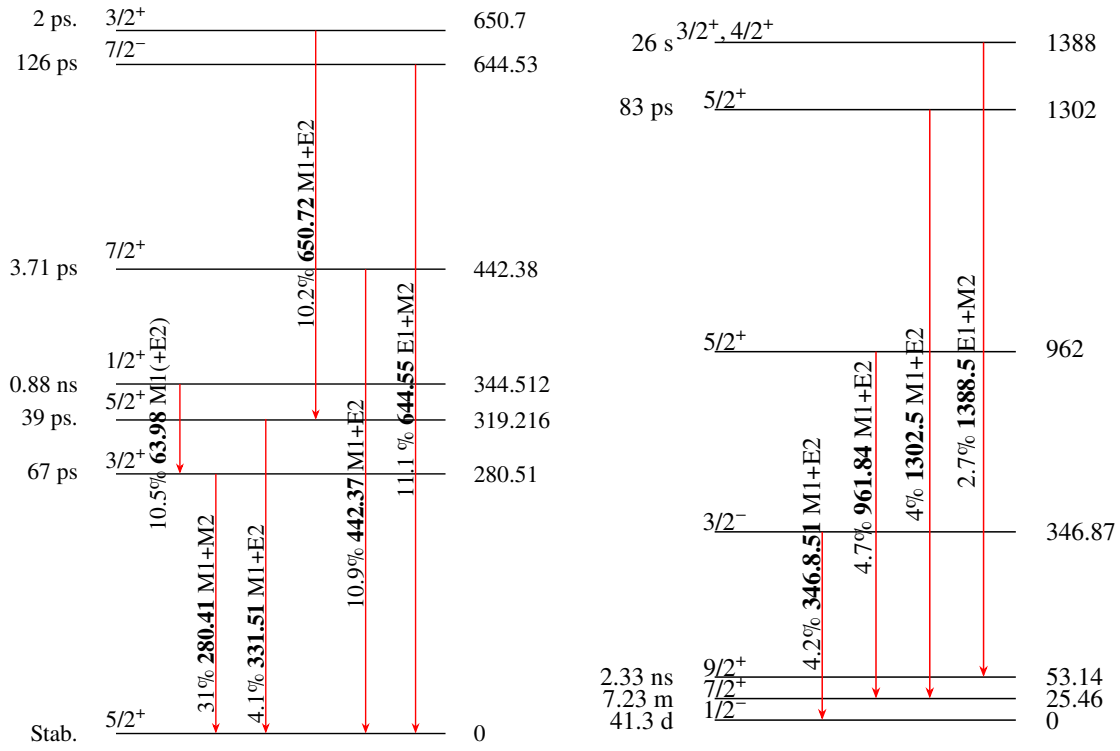

Figure 2: Nuclear decay schemes of ^{105}Ag and ^{105}Cd, with energy levels (keV), transitions, spin-parity values, and branching ratios

The activity of the ^{105}Cd radionuclide ($T_{1/2}$ = 55.5 min) was determined using γ-rays at 346.87 keV (4.2%), 961.84 keV (4.69%), and 1302.46 keV

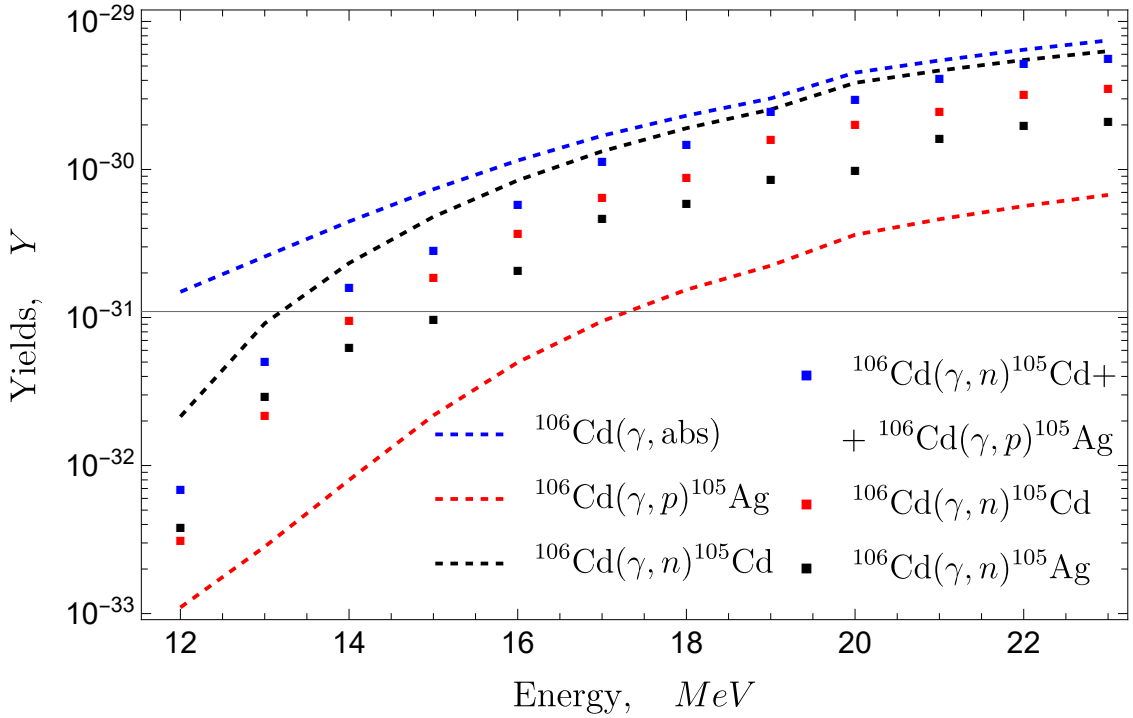

Figure 3: The yields for the ^{106}Cd(γ, n)^{105}Cd and ^{106}Cd(γ, p)^{105}Ag reactions are plotted as a function of bremsstrahlung end-point energy, displaying experimental results from this work (solid rectangles) alongside simulated values obtained using the TALYS (dashed lines)

(4.20%). The ^{105}Ag radionuclide exists in both isomeric and ground states. The isomeric state, ^{105m}Ag ($T_{1/2}$ = 7.23 min), has a short half-life, making its activity measurement infeasible. For the ground state, ^{105g}Ag ($T_{1/2}$ = 41.29 d), interference-free γ-rays at 63.98 keV (10.5%), 280.41 keV (30.2%), 344.52 keV (41%), and 644.55 keV (11.1%) were used for activity measurement. Since ^{105m}Ag decays to ^{105g}Ag with a 99.66% internal transition (IT) coefficient, and ^{105}Ag is produced both directly via photonuclear reactions and through the decay of the parent ^{105}Cd ($T_{1/2}$ = 55.5 min), the measured γ-ray activity reflects the cumulative contribution of $^{105}(0.9966m + g)$Ag + ^{105}Cd. To isolate the activity of ^{105}Ag, spectra were analyzed 9 hours post-irradiation (equivalent to 10 half-lives of ^{105}Cd), assuming complete decay of ^{105}Cd to ^{105}Ag.

Fig. 3 and Table. 3 show the yields of the (γ, n) and (γ, p) reactions on the nucleus ^{106}Cd. Due to the absence of published data, these measurements were compared only with theoretical calculations. While individual theoretical yields for the (γ, n) and (γ, p) reactions, calculated using the TALYS code, deviate significantly from experimental values, their combined theoretical yield closely matches the total experimental yield. This suggests that the overall photoabsorption yield calculated by TALYS is reliable, with differences primarily arising from a redistribution of the total yield between

Table 3: Experimental results of the yields Y_{exp} for the $^{106}Cd(\gamma, n)^{105}Cd$ and $^{106}Cd(\gamma, p)^{105}Ag$ reactions

Energy, MeV	$Y_{exp}, \times 10^{-30}$		
	^{105}Cd	^{105}Cd + ^{105} Ag	^{105}Ag
12	0.0038 ± 0.0004	0.0068 ± 0.0007	0.0031 ± 0.0004
13	0.029 ± 0.003	0.050 ± 0.006	0.021 ± 0.002
14	0.062 ± 0.006	0.16 ± 0.02	0.09 ± 0.01
15	0.09 ± 0.01	0.28 ± 0.03	0.18 ± 0.02
16	0.21 ± 0.02	0.57 ± 0.06	0.36 ± 0.04
17	0.46 ± 0.05	1.1 ± 0.1	0.64 ± 0.07
18	0.58 ± 0.06	1.4 ± 0.2	0.87 ± 0.09
19	0.84 ± 0.01	2.4 ± 0.3	1.54 ± 0.01
20	0.97 ± 0.01	2.9 ± 0.3	2.0 ± 0.2
21	1.6 ± 0.2	4.0 ± 0.4	2.4 ± 0.3
22	1.9 ± 0.2	5.1 ± 0.6	3.2 ± 0.4
23	2.1 ± 0.2	5.6 ± 0.6	3.5 ± 0.4

the (γ, n) and (γ, p) channels. However, differences in reaction thresholds imply that the total photodisintegration rate may still be inaccurate, as energy dependence directly influences reaction rates.

Fig. 4 shows the ratios of the experimentally obtained to the theoretically calculated reaction yields, $Y^{\text{nat}}_{\text{exp}}/Y^{\text{nat}}_{\text{TALYS}}$, for the (γ, n) and (γ, p) reactions on ^{106}Cd. These ratios provide a direct comparison between experimental data and the predictions based on the statistical nuclear-reaction models implemented in the TALYS code.

From the results presented, it is evident that the experimentally measured yields confirm and reinforce the conclusions drawn in Refs. [16, 17], namely, that there exist substantial and systematic differences between the calculated and observed values of both the (γ, n) and (γ, p) yields.

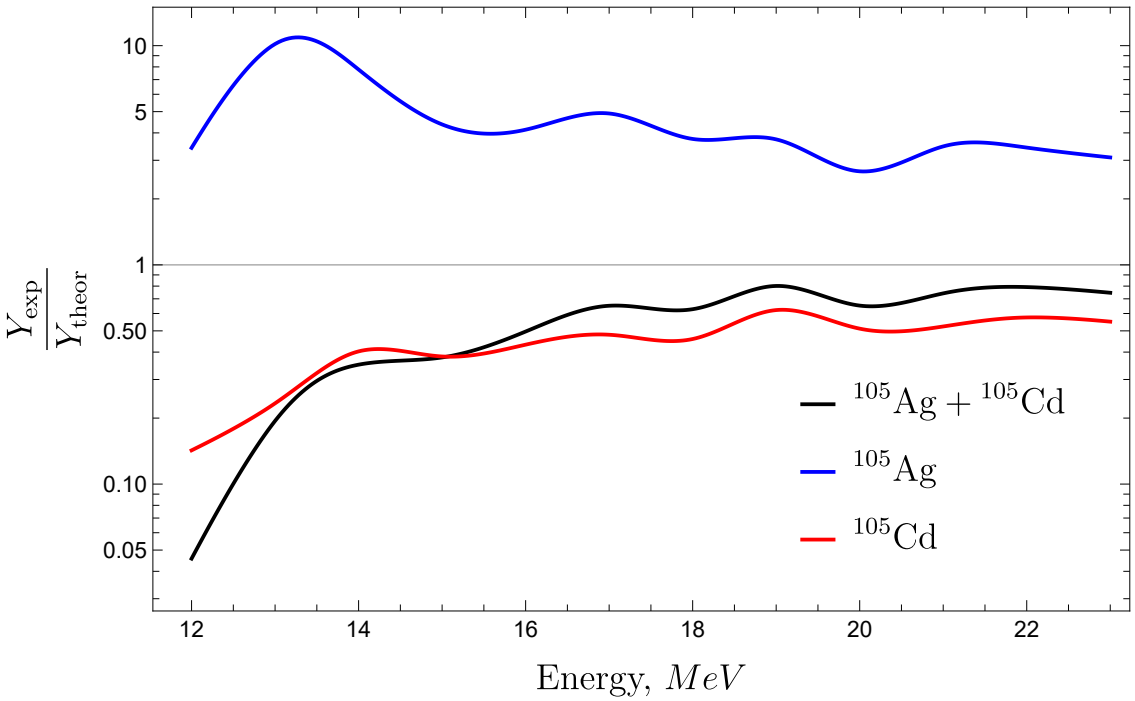

Figure 4: The experimental and theoretical values of the ratio for the yields of the (γ,p) and (γ,n) reactions

3.2 ^{106}Cd in nucleosynthesis processes

The nucleosynthesis of ^{106}Cd offers critical insights into the astrophysical processes driving the formation of p-nuclei, which primarily arise through photodisintegration pathways rather than the conventional s- or r-processes. The stable isotope ^{106}Pd serves as a significant barrier, blocking neutron capture pathways and underscoring the importance of alternative mechanisms, such as photoneutron emission. Notably, the ^{108}Cd$(\gamma, 2n)^{106}$Cd reaction highlights the role of double neutron emission under high-energy photon conditions prevalent in explosive astrophysical settings, such as supernovae or gamma-ray bursts.

Analysis of flux percentages reveals that the (γ, n) pathway, contributing 55.8%, dominates but may involve exotic processes or potential mislabeling in flux diagrams, necessitating further experimental validation. The (γ, p) reaction, with a 15.7% flux and a 7.35 MeV threshold, competes closely with neutron emission, while the (γ, α) channel, at 3.8% and a 1.63 MeV threshold, plays a minor yet notable role in isotopic destruction. Together, these reactions shape the evolution of ^{106}Cd, providing a window into the conditions of nucleosynthesis sites. Ongoing efforts aim to refine flux measurements using advanced detector systems and computational models to better constrain the astrophysical parameters favoring p-process dominance.

The flux diagram (Fig. 5) illustrates a complex interplay between produc-

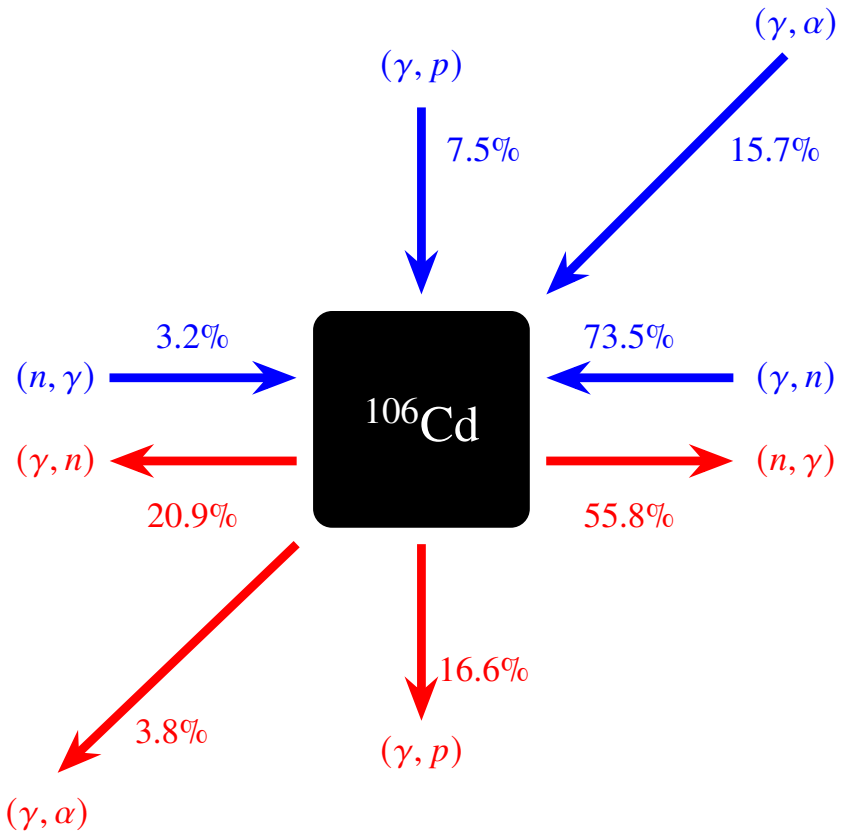

Figure 5: Cumulative nucleosynthesis fluxes governing the synthesis and annihilation of the isotope ^{106}Cd. The production fluxes are standardized to 100%, with destruction fluxes proportionally adjusted using the same normalization factor. Fluxes contributing less than 1% are omitted from the representation.

tion and destruction channels. The primary production pathway, photodisintegration of ^{107}Cd, significantly contributes to the net yield of ^{106}Cd, with total production fluxes (100%) exceeding destruction fluxes. This imbalance suggests that ^{106}Cd accumulates over time in these environments, aligning with observed p-nuclei abundances in meteoritic materials. Destruction channels, including (γ, n), (γ, p), and (γ, α), are governed by their respective energy thresholds, with (γ, n) being the most energetically favorable at 10.87 MeV.

This unexpected prevalence of the (γ, p) channel is attributed to the shell structure of ^{106}Cd, with 48 protons and 58 neutrons, near the $Z = 50$ proton shell closure. This proximity possibly boosts proton emission via specific single-particle states or reduced Coulomb barriers, while neutron emission may be suppressed by lower level density or higher neutron separation energy. The TALYS statistical models, based on the Hauser-Feshbach formalism, overlook these shell effects, resulting in significant underpredictions for both channels. These results underscore the importance for refined theoretical models, possibly incorporating shell-model calculations or adjusted level

densities parameters, and further experiments to better understand nucleosynthesis in ^{106}Cd.

From the perspective of nucleosynthesis, particularly the production of p-nuclei, this result is of considerable importance. It should be noted that, for the bypassed cadmium isotopes involved in the p-process, there are no direct experimental measurements of the yields of the photoneutron and photoproton reactions. In Ref. [17], the photodisintegration reactions on ^{106}Cd are analyzed in the context of the production of bypassed nuclei in the p-process, highlighting the need for more accurate experimental data to constrain theoretical models.

Theoretical reaction yields serve as the primary input for calculating the photonuclear reaction rates λ for the cadmium isotopes ^{106,108}Cd [18, 19]. Since these reaction rates are directly employed in nucleosynthesis network simulations, any inaccuracy in the theoretical yields propagates into the predicted astrophysical reaction rates. Consequently, such errors may lead to significant deviations in the calculated abundances of nuclei synthesized in stellar environments. This issue becomes particularly relevant for the p-process of nucleosynthesis, where small changes in the photodisintegration rates of key isotopes can produce disproportionately large variations in the final abundances of p-nuclei.

In that study, it was demonstrated that an error of one order of magnitude in the photonuclear reaction rate λ for reactions involving p-nuclei—particularly those that drive their photodisintegration or photo-erosion—can alter their final abundances by a factor of five to six in a core-collapse (Type II) supernova model. This finding emphasizes that even seemingly moderate differences between theoretical and experimental reaction yields may have profound astrophysical consequences.

Furthermore, the deviations observed between experimental data and the TALYS predictions are not merely statistical fluctuations but are possibly connected to nuclear-structure effects, such as shell closures and the detailed level densities of ^{106}Cd. These nuclear-structure features are often insufficiently treated in purely statistical models, which approximate nuclear properties by averaged quantities. As a result, the (γ, p) and (γ, n) reaction yields may be redistributed in a manner not captured by the theoretical calculations, leading to the mismatches observed in Fig. 4.

Therefore, in order to improve the reliability of nucleosynthesis models—particularly for the production of p-nuclei—it is essential to obtain more precise experimental data for photonuclear reactions on ^{106,108}Cd and other isotopes in this mass region. Such experimental constraints would enable refinements of the input nuclear physics in reaction codes like TALYS, reduce the uncertainties in the calculated reaction rates λ, and ultimately improve our understanding of the role of cadmium isotopes in the p-process.

Fig. 6 presents the temperature-dependent behavior of the ratio $\lambda_{\mathrm{TAL}}/\lambda_{\mathrm{cr}}$, which quantifies the discrepancy between two calculated photodisintegration rates for the isotope ^{106}Cd in the context of the p-process nucleosynthesis. Here, λ_{TALYS} denotes the photodisintegration rate derived using the TALYS nuclear reaction code, a widely used computational tool for modeling photon-induced nuclear reactions. This rate is computed as the cumulative contribution of individual reaction channels, encompassing both single-nucleon and multi-nucleon photonuclear processes. Specifically, it includes reactions leading to the emission of up to two nucleons, such as photoneutron (γ, n), photoproton (γ, p), two-neutron $(\gamma, 2n)$, neutron-proton (γ, np), and two-proton $(\gamma, 2p)$ emissions, as well as deuteron (γ, d) and alpha (γ, α) emissions. The expression for λ_{TALYS} is given by:

$$\lambda_{\mathrm{TALYS}} = \lambda_\alpha + \lambda_d + \lambda_n + \lambda_p + \lambda_{2n} + \lambda_{np} + \lambda_{2p} \tag{3}$$

In contrast, λ_{corr} represents a refined photodisintegration rate obtained by adjusting λ_{TALYS} to incorporate experimental data on the yields of photoneutron and photoproton reactions. This correction accounts for differences between theoretical predictions and experimental measurements by scaling the contributions of the (γ, n) and (γ, p) channels using the ratio of experimental to theoretical reaction yields for a natural isotopic composition. The corrected rate is expressed as:

$$\lambda_{\mathrm{corr}} = \lambda_\alpha + \lambda_d + \frac{Y_{\mathrm{exp}}(\gamma, n)}{Y_{\mathrm{theor}}(\gamma, n)}\lambda_n + \frac{Y_{\mathrm{exp}}(\gamma, p)}{Y_{\mathrm{theor}}(\gamma, p)}\lambda_p + \lambda_{2n} + \lambda_{np} + \lambda_{2p} \tag{4}$$

The correction applied in λ_{corr} is an approximation, primarily due to the limited availability of high-resolution experimental data for the yields of individual photonuclear reactions. Despite this limitation, two key physical insights justify its use. First, at temperatures up to 10×10^9 K (commonly denoted as $T_9 = 10$), the photon Planck spectrum, which governs the energy distribution of incident photons in astrophysical environments, overlaps significantly with the yields of the (γ, n) and (γ, p) reactions. This overlap occurs in the energy range from the nucleon emission threshold of approximately 7.4 MeV to about 15–16 MeV, where the Giant Dipole Resonance (GDR) reaches its maximum. The GDR is a collective nuclear excitation mode that dominates photon absorption in this energy range, making it critical for accurate rate calculations. Second, the energy window for single-nucleon reactions, such as (γ, n) and (γ, p), is constrained to approximately 20 MeV. Beyond this, starting at an energy of 12.3 MeV, thresholds for multi-nucleon reactions (e.g., $(\gamma, 2n)$, (γ, np) open, and these processes dominate the reaction yields at higher energies due to their larger phase space.

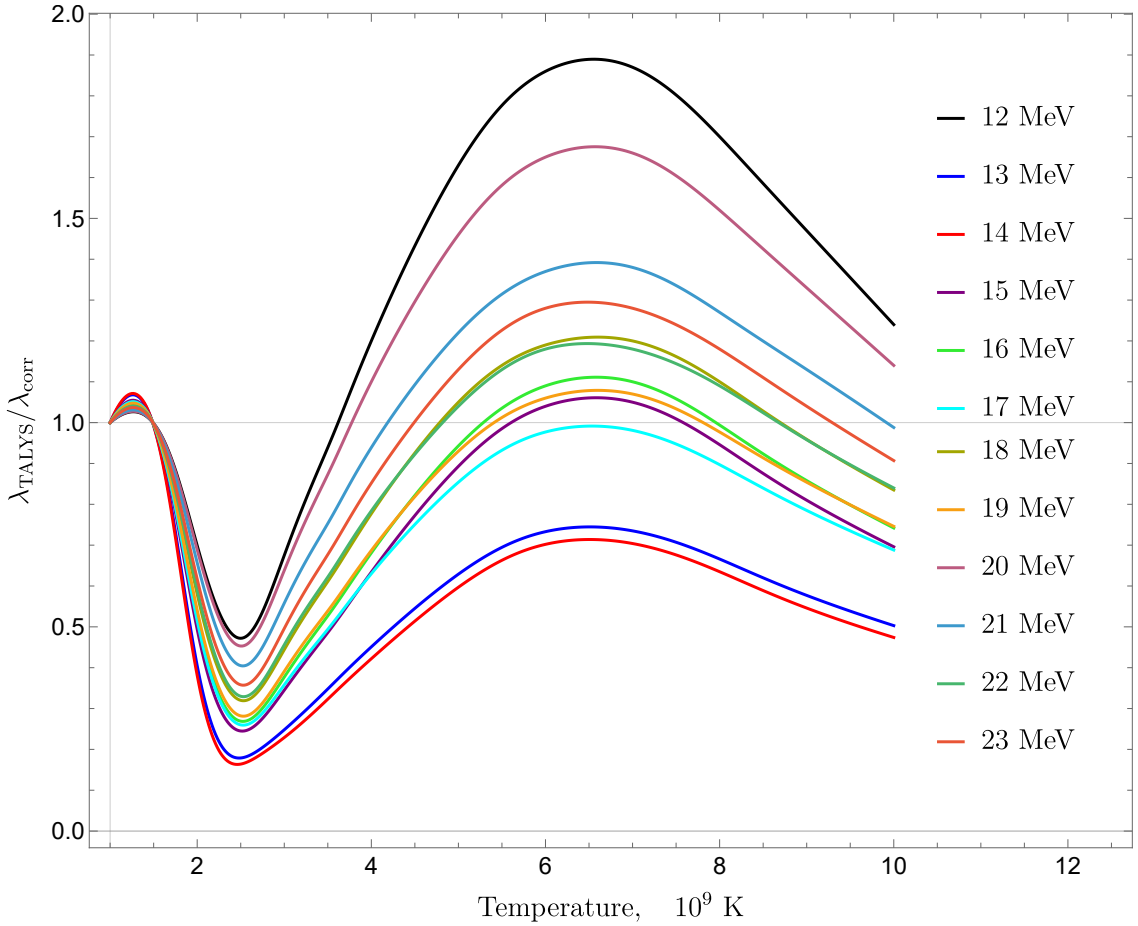

Figure 6: The ratio $\lambda_{\mathrm{TALYS}}/\lambda_{\mathrm{corr}}$ compares the photodisintegration reaction rates for the isotope ^{106}Cd. Here, λ_{TALYS} represents the rate calculated using the TALYS code, while λ_{corr} denotes the rate obtained after normalizing the yields to align with experimental the yields. This ratio illustrates the difference between theoretical predictions and experimentally adjusted reaction rates.

The use of a bremsstrahlung spectrum with endpoint energies ranging from 13 to 23 MeV provides a reasonable approximation for modeling the photodisintegration of ^{106}Cd in the p-process, a nucleosynthesis mechanism responsible for producing proton-rich isotopes. In the temperature range of $T_9 = 1.5$ to 4, typical of p-process environments, calculations based on the TALYS code tend to underestimate the photodisintegration rate of ^{106}Cd. This underestimation arises because the theoretical yields may not fully capture the experimental behavior of the (γ, n) and (γ, p) reactions. Conversely, at higher temperatures ($T_9 > 4$), the TALYS calculations risk overestimating the photodisintegration rate, as the contributions from multi-nucleon channels become more significant and may be exaggerated in the model. Such differences have profound implications for nucleosynthesis models, as they can lead to inaccuracies in predicting the final abundance of ^{106}Cd, a key p-process isotope.

Accurate modeling of these rates is essential for understanding the production of heavy elements in stellar environments, such as Type II supernovae or explosive nucleosynthesis scenarios.

Conclusion

A thorough experimental investigation of the photodisintegration of ^{106}Cd, a proton-rich isotope pertinent to p-process nucleosynthesis, carried out at Dubna during the Summer Session 2025, is presented in this document. The importance of p-nuclides, which are produced through photodisintegration reactions such as (γ, n), (γ, p), and (γ, α) in high-temperature astrophysical environments, like supernovae, is described in the introduction. It draws attention to discrepancies between computed and observed p-nuclide abundances, especially for cadmium isotopes, caused by uncertainties in photonuclear cross-sections and nuclear composition.

The experimental setup, which is described in the "Materials and Methods" section, exposed natural cadmium targets to electron energies ranging from 10 to 23 MeV using the MT-25 microtron to produce bremsstrahlung radiation. A high-purity germanium detector was used to measure the gamma-ray emissions from activated isotopes. The yields were computed and compared to theoretical predictions. The study used Geant4 simulations to model the bremsstrahlung spectrum and carefully controlled the beam parameters. The ^{106}Cd$(\gamma, n)^{105}$Cd and ^{106}Cd$(\gamma, p)^{105}$Ag reactions are the main focus of the results. While ^{105}Ag yields exceeded theoretical estimates, experimental yields for ^{105}Cd fell short of TALYS predictions, indicating flaws in statistical models, especially because of shell effects close to $Z = 50$. Implications for nucleosynthesis are examined, with a focus on the function of ^{106}Cd in p-process pathways and the influence of reaction rate uncertainties on abundance forecasts. The dominance of photoneutron emission and the unexpected importance of the (γ, p) channel are depicted in flux diagrams.

The study concludes that improved experimental data and refined nuclear models, incorporating shell effects and level densities adjustments, are essential for accurate p-process modeling, with significant implications for understanding heavy element formation in stellar environments.

0.1 Acknowledgments

I sincerely thank my supervisor Rasulova Fazilat, and the staff at JINR's FLNR for their guidance during this project. I also acknowledge the JINR Summer Student Programme for providing this opportunity and financial support, including travel reimbursement, accommodation, and daily allowances.

References

[1] M. Arnould and S. Goriely. "The p-process of stellar nucleosynthesis: astrophysics and nuclear physics status". In: *Physics Reports* 384.1 (2003), pp. 1–87. DOI: 10.1016/S0370-1573(03)00242-4.

[2] W. R. Hix and F.-K. Thielemann. "Computational methods for nucleosynthesis and nuclear energy generation". In: *Journal of Computational and Applied Mathematics* 109.1-2 (1999), pp. 321–351. DOI: 10.1016/S0377-0427(99)00163-6.

[3] Y. Xu et al. "The p-process in stellar nucleosynthesis: current status and problems needing resolution". In: *Astronomy & Astrophysics* 549 (2013), A106. DOI: 10.1051/0004-6361/201220537.

[4] R. H. Cyburt et al. "The JINA REACLIB Database: Its Recent Updates and Impact on Type-I X-ray Bursts". In: *Astrophysical Journal Supplement Series* 189.1 (2010), pp. 240–252. DOI: 10.1088/0067-0049/189/1/240.

[5] A. Lepretre et al. "Photoneutron cross sections of Cd isotopes". In: *Nuclear Physics A* 219.1 (1974), pp. 39–60. DOI: 10.1016/0375-9474(74)90569-9.

[6] R. Capote et al. "RIPL - Reference Input Parameter Library for Calculation of Nuclear Reactions and Nuclear Data Evaluations". In: *Nuclear Data Sheets* 110.12 (2009), pp. 3107–3214. DOI: 10.1016/j.nds.2009.10.004.

[7] S. S. Belyshev et al. "Photonuclear reactions on cadmium isotopes". In: *Physics of Atomic Nuclei* 77.6 (2014), pp. 809–818. DOI: 10.1134/S1063778814060056.

[8] S. S. Belyshev et al. "Photodisintegration of cadmium isotopes near the neutron separation energy". In: *Physics of Atomic Nuclei* 76.8 (2013), pp. 931–939. DOI: 10.1134/S1063778813080042.

[9] D. Savran, T. Aumann, and A. Zilges. "Experimental studies of the Pygmy Dipole Resonance". In: *Progress in Particle and Nuclear Physics* 70 (2013), pp. 210–245. DOI: 10.1016/j.ppnp.2013.02.003.

[10] O.D. Maslov and S.N. Dmitriev. *Use of MT-25 microtron for scientific and applied investigations*. https://inis.iaea.org/collection/NCLCollectionStore/_Public/35/022/35022466.pdf. Accessed: 2025-07-24.

[11] S.S. Belyshev, A.N. Ermakov, B.S. Ishkhanov, et al. "Studying photonuclear reactions using the activation technique". In: *Nuclear Instruments and Methods in Physics Research Section A: Accelerators, Spectrometers, Detectors and Associated Equipment* 745 (2014), p. 133. DOI: 10.1016/j.nima.2014.01.057.

[12] V.V. Varlamov et al. "Reliability of the data on the cross sections of the partial photoneutron reaction for 63,65Cu and 80Se nuclei". In: *Bulletin of the Russian Academy of Sciences: Physics* 80 (2016), pp. 317–324. DOI: 10.3103/S1062873816030333.

[13] S. Agostinelli, J. Allison, K. Amako, et al. "Geant4 – a simulation toolkit". In: *Nuclear Instruments and Methods in Physics Research Section A: Accelerators, Spectrometers, Detectors and Associated Equipment* 506 (2003), p. 250. DOI: 10.1016/S0168-9002(03)01368-8.

[14] B.S. Ishkhanov and A.A. Kuznetsov. "The mass distribution of 238U photofission fragments". In: *Moscow University Physics Bulletin* 68 (2013), p. 279. DOI: 10.3103/S0027134913040073.

[15] S.S. Belyshev et al. "Measuring nuclear reaction yields in a procedure based on decay chain analysis". In: *Moscow University Physics Bulletin* 66 (2011), p. 363. DOI: 10.3103/S0027134911040059.

[16] S. S. Belyshev, B. S. Ishkhanov, A. A. Kuznetsov, et al. "Photodisintegration of cadmium isotopes". In: *Physics of Atomic Nuclei* 77 (2014), pp. 809–816. DOI: 10.1134/S1063778814060039.

[17] S. S. Belyshev, A. A. Kuznetsov, K. A. Stopani, et al. "Photonuclear reactions on the cadmium isotopes 106,108Cd at the bremsstrahlung endpoint energy of 55.5 MeV". In: *Physics of Atomic Nuclei* 79 (2016), pp. 641–647.

[18] Y. Xu et al. "Databases and tools for nuclear astrophysics applications". In: *Astronomy and Astrophysics* 549 (2013), A106. DOI: 10.1051/0004-6361/201220537.

[19] R. H. Cyburt, A. M. Amthor, R. Ferguson, et al. "The JINA REACLIB database: its recent updates and impact on type-I X-ray bursts". In: *The Astrophysical Journal Supplement Series* 189 (2010), p. 240. DOI: 10.1088/0067-0049/189/1/240.